Seismically driven characterization of vuggy porosity and fractures in a carbonate field, Sirte Basin, Libya

Mahdi Hammad,[1] Abdulhamed Shahlol,[1] Sobhi Hajaj,[1] Amares Aoues,[2] Ahmed Ouenes,[2*] Hamed El Werfali,[1] Fawzi BuArgoub[1] and Anthony Kirkham[3] describe a workflow that fully utilizes pre-stack seismic attributes to derive reliable geologic and fracture models for a carbonate field in the Sirte Basin, Libya, validated by blind well testing and actual wells drilled after the study.

The first step in the workflow is to run post-stack seismic processes, which includes volumetric curvature, high resolution post-stack inversion and spectral imaging. The second step consists of using the various post-stack seismic cubes to derive 3D geologic models constrained by multiple seismic attributes. The third step consists of using the various post-stack seismic cubes and the derived geologic models to build predictive fracture models validated with wells not used during the modelling effort.

This workflow was applied to a complex Paleocene fractured carbonate field in the Sirte basin, Libya. A large number of post-stack seismic attributes were generated in time and then depth converted within a 3D geocellular grid. These seismic attributes were used simultaneously to create geologic and fracture models. The resulting porosity, and fracture density models were validated during the study with a blind well and after the study with a newly drilled well.

Introduction

The characterization of fractured reservoirs remains a challenging task for most E&P and service companies. The main difficulty when characterizing these reservoirs is how to account for the lateral and vertical variations of fracture density in the interwell region. In exploration, where limited well data is available, this difficulty is aggravated and the only solution is to rely heavily on the use of seismic data. Given that the availability of wide azimuth seismic surveys remains rare in Libya, the use of azimuthal anisotropy technologies is not an option and one needs to rely solely on narrow azimuth surveys. When searching for proven workflows to characterize fractured reservoirs, one can notice that most of the current fractured reservoir modelling technologies do not fully utilize the rich information available in the seismic data, thus their poor predictive capabilities. The weakness of these fractured modelling technologies is apparent in the various publications and presentations where model validation with blind well tests and actual drilling is always missing (Akram et al., 2010).

One interesting approach is the continuous fracture modelling (CFM) (Ouenes, et al., 1995; Ouenes, 2000) which relies heavily on the use of multiple seismic attributes. The ability of the CFM approach to use simultaneously a multitude of seismic attributes leads to predictive fracture models demonstrated with many blind wells, actual drilling, and reservoir simulation models (Bejaoui et al., 2010; Christensen et al., 2006; Jenkins et al., 2009; Pinous et al., 2006; Laribi et al., 2004; Ross et al., 2009, Ouenes et al., 2008, Ouenes et al., 2010; Zellou et al., 2006). The CFM approach is applied to a complex fractured carbonate field in the Sirte basin, Libya, where a detailed fracture density model was built in 3D and validated with a blind well during the study and a newly drilled well selected based on the study results.

Geologic observations

The considered field is located in the Sirte Basin where the Soluq and Agedabiah Depressions adjoin each other. The initial exploration effort used 2D seismic lines and led to the discovery of oil in 1996. Following this discovery, a 325 km^2 3D seismic narrow azimuth survey was acquired. Exploration efforts restarted in 2007 with the drilling of seven additional wells which targeted and encountered the Paleocene Dolomite reservoir. The depth structure map at the Top Paleocene is shown in Fig. 1.

The Paleocene Dolomite reservoir is the result of major geologic events that affected the Sirte Basin. Abadi et al. (2008) provides a good summary of these major events. The reservoir comprises the Palaeocene Dolomite which unconformably overlies the Cretaceous Kalash Limestone Fm. At the southern end of the field, the Palaeocene Dolomite is

[1] *Arabian Gulf Oil Company (AGOCO), Libya.*
[2] *Prism Seismic, USA.*
[3] *Sedimentology & Reservoir Development, UK.*
[*] *Corresponding author, E-mail: ouenes@prismseismic.com*

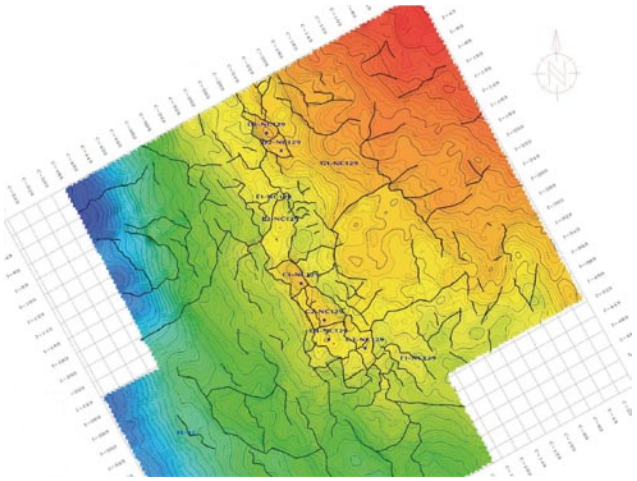

Figure 1 *Structural depth map at the Top Paleocene. Two newly drilled wells were not used in the modelling effort.*

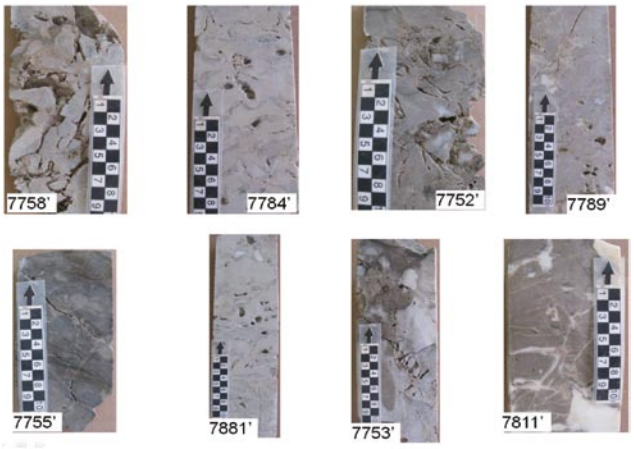

Figure 2 *Examples of core porosities from multiple wells showing vuggy, channel, and fracture porosities. Some fractures are cemented with anhydrite as seen in bottom right photograph.*

overlain by the Eocene Antelat Fm. which is variably dolomitic and in turn overlain by the Eocene Lower Shale Fm. In most of the wells the Palaeocene Dolomite is directly overlain by the Lower Shale Fm. and assumed to be unconformable.

The examination of various cores indicates that virtually all porosity is secondary in the form of vugs and fractures. Essentially no primary inter-granular porosity has survived and very little inter-crystalline porosity exists despite the extensive dolomite replacement. The vugs vary in size from pin-point to several centimetres across. Fig. 2 illustrates the range of visible and microscopic porosity types. Open fractures could be either completely or partially cemented and could also have been widened by leaching. Other fractures may be compaction features related to pressure solution along stylolites or subsidence features related to karstification at deeper levels.

All the cores have been severely affected diagenetically to the extent that essentially all the porosity appears to be secondary and most of the reservoir interval has been either leached or dolomitized.

The leaching led to the formation of three basic types of vugs: isolated vugs, large connected vugs, and enlarged fractures. A later leaching phase which post-dated the unconformity affected the fracture system even in the Antelat Fm. Such leaching could have helped increase the sizes of pre-existing moulds and improved their connectivity, enlarged fracture apertures, and created channels or fissures.

Although no bit-drops have been recorded to indicate cavernous porosity, there is a suggestion of crackle fracturing at one well which could indirectly indicate incipient collapse into major void space not far beneath the top Paleocene unconformity.

Fractures are relatively common in most cores but have generally been enlarged, often to the extent that the fractures became almost indistinct or were transformed into channels (fissures) by the same dissolution process that created mouldic porosity and vugs in the adjacent rock matrix. The productivity of some of the wells is essentially governed by the various types of vuggy porosity. On the other hand, other wells noticeably lack vuggy porosity and productivity is governed by open or partially cemented fractures.

The challenge in this field is to use the limited well data to model accurately the vuggy porosity and fracture density in order to plan additional drilling locations. To meet this challenge, AGOCO will rely on the use of seismic data and advanced seismically driven reservoir modelling technologies and workflows available in CRYSTAL, Prism Seismic geomodelling software.

Workflow overview

The workflow used in this project is different from the common industry workflow where seismic data is mainly used for structural interpretation which leads to seismic horizons that are depth converted, then used to build a structural framework in the depth domain. The workflow used in this project moves the centre of gravity to the geophysics where most of the efforts are spent in the time domain and the value of the seismic data is fully utilized. The workflow starts by using the interpreted horizons and faults to build in the time domain a water tight structural framework and a 3D geocellular grid. The first step in this workflow consists of generating post-stack seismic attributes through the use of volumetric curvature, spectral imaging, and high resolution post-stack seismic inversion. The various 3D seismic cubes are snapped to the 3D geoecellluar grid in the time domain and become available in a stratigraphic framework. The 3D geocelluar time grid and its various snapped seismic attributes are depth converted. Once in depth, the seismic attributes are used to build seismically constrained geologic models. The final step will use both the seismic attributes and the derived geologic models to construct 3D fracture models which are validated with blind wells. The details of this workflow are described below.

Geophysical modelling

The use of seismic data in reservoir modelling involves seismic resolution enhancement, seismic-well ties, volumetric curvature, spectral imaging, and high resolution post-stack inversions. The key to successful use of seismic attributes in reservoir modelling is to generate attributes that are related to rock and fluid distribution and to be able to constrain the geologic and fracture models to a multitude of seismic attributes.

Prior to initiating the reservoir modelling effort, one needs to ensure that the processed seismic data is optimized. Most of these optimizations efforts are done during the seismic processing step, but sometimes more can be done on the final post-stack data. One of the steps that could be applied to the final processed seismic is the post-stack resolution enhancement. This rapid and efficient process could add 10 Hz or even more to the dominant frequency. In this project, the resolution enhancement (Mundim et al., 2006) was applied to the post-stack seismic and led to a substantial boost of frequencies between 30 and 60 Hz thus increasing the dominant frequency by at least 15 Hz as shown in Fig. 3. This increase in resolution will be very beneficial for the structural interpretation, the well ties, and the generation of seismic attributes.

Using the enhanced seismic, the workflow starts with the well ties at all the wells. Synthetics were built at eight wells. When comparing the well ties performed with the original seismic to the ones performed with the enhanced seismic, we noticed an improvement of 10% or more in the correlation coefficient thus confirming the benefits of the resolution enhancement.

The use of volumetric curvature (Al-Dosari and Marfurt, 2006), which is making obsolete curvature methods applied to surfaces and coherency type seismic attributes, provided some of the best seismic attributes for imaging the complex fault system. Volumetric curvature provides many seismic attributes able to highlight peaks (most negative curvature), valleys (most positive curvature), and other key structural features. In the considered field the most negative curvature shown in Fig. 4 is one of the best volumetric curvature attribute used to image the faults.

The next seismic process applied to the enhanced seismic is spectral imaging. Spectral imaging is a workflow that allows the examination of the seismic data in specific frequency ranges. The resulting seismic attributes are frequency dependent or represent statistical properties that describe the behaviour of the seismic power spectrum at different frequencies. Many of the seismic attributes derived from spectral imaging reflect variations in fluid and rock properties, but they remain rarely used in reservoir modelling.

Most geophysicists are familiar with the frequency dependent attributes (Partyka et al., 1999) that could be useful in imaging many geologic features. However, using the wavelet transform instead of the Fast Fourier Transform, the statistical spectral attributes computed in

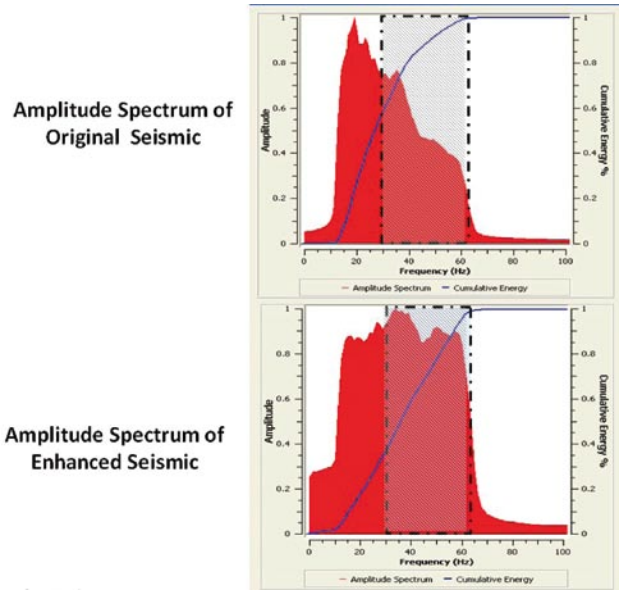

Figure 3 *Amplitude spectrum before and after applying the seismic resolution enhancement. Notice the boost in amplitude in the 30 to 60 Hz range.*

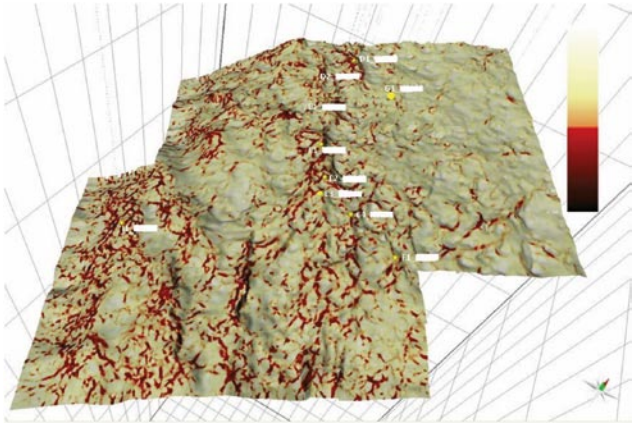

Figure 4 *Most negative curvature extracted along the top Paleocene time horizon.*

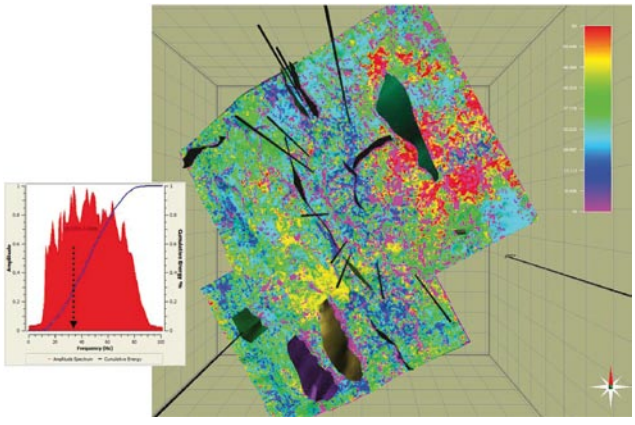

Figure 5 *Tuning frequency extracted along the top Paleocene time horizon.*

this project provided better attributes that were sensitive to facies and other geologic changes. One of these attributes is the tuning frequency which provides at each sample the frequency at which tuning occurs. Fig. 5 shows the tuning frequency in the considered field.

The final post-stack seismic process is the inversion. Various inversion algorithms are available and they serve multiple purposes. These inversions are divided into two categories: deterministic and stochastic. For example, the fast coloured inversion (Lancaster and Whitcombe, 2000) is a deterministic inversion used mainly for interpreting horizons. Another deterministic seismic inversion is the generalized linear inversion (GLI) (Cooke and Schneider, 1983) that provides better resolution than the coloured inversion. For reservoir and fracture modelling where vertical resolution is critical, the stochastic inversion (Haas and Dubrule, 1994) remains the best approach since it provides the means to derive an impedance model at a resolution of 0.5 ms to 1 ms needed for the geologic and fracture modelling.

Prior to any seismic inversion, a water tight structural framework is needed to account for the faults and their offsets. For this field, three horizons and 120 faults (Fig. 6) were used to build the structural framework in the time domain.

Given the structural framework and the well ties, the GLI inversion was run first (Fig. 7) followed by the stochastic inversion (Fig. 8) which uses the GLI impedance as a soft constraint. Blind wells were used to evaluate various realizations of the stochastic impedance and the best realization was kept for the geologic and fracture modelling.

To be able to use the seismic attributes in geologic and fracture modelling, a 3D geocellular grid is built in the time domain. The derived structural framework is divided into rectangular cells that are 70 m x 70 m in the areal direction and about 1 ms in the vertical direction where 60 conformable layers are used to capture the vertical heterogeneities. The resulting 3D geocellular grid has 4.6 million cells. With the 3D geologic grid available in the time domain, all the derived seismic attributes could be snapped or resampled and made available to the geologic and fracture modelling upcoming effort.

The final step before starting the geologic and fracture modelling effort is the conversion to depth of the 3D geocellular grid. This is achieved by using an average velocity at the top of the 3D grid and an interval velocity defined in every cell of the 3D geocellular grid in time. This time-to-depth conversion will provide an equivalent 3D geocellular grid in the depth domain along with all the snapped seismic attributes. Fig. 9 shows the selected impedance from the stochastic inversion in the 3D geocellular depth grid.

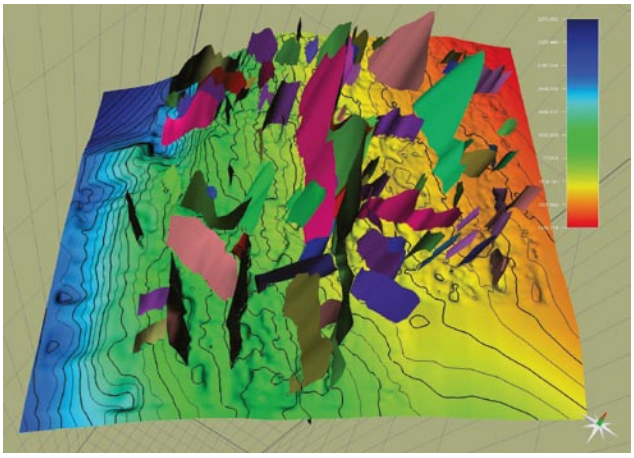

Figure 6 *Three horizons and 120 faults were used to build a water tight structural framework in the time domain. The structural framework is needed for the seismic inversion and to build a 3D geocellular grid in the time domain.*

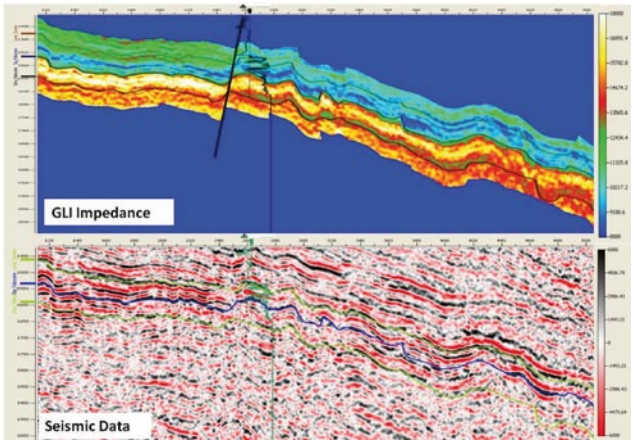

Figure 7 *GLI impedance along an inline as compared to the original seismic data. Notice in the impedance the clean fault offset near the well which is the result of using the structural framework able to account for all the faults. Other faults exist on this section and were accounted for in the structural framework.*

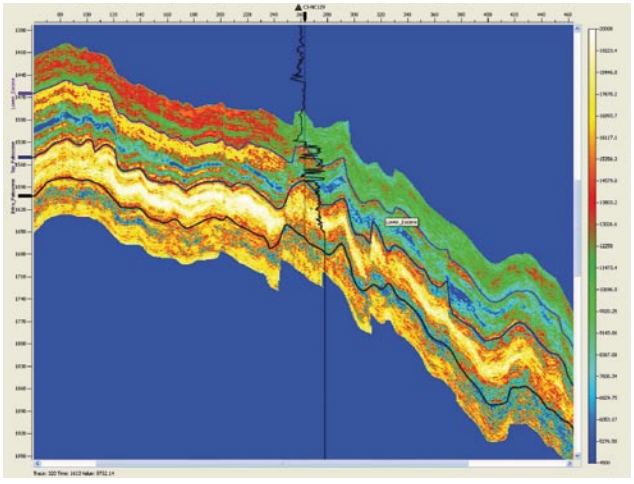

Figure 8 *One realization of the stochastic impedance along an inline. Notice the higher vertical resolution while still honouring the trends seen in the GLI impedance used as a soft constraint.*

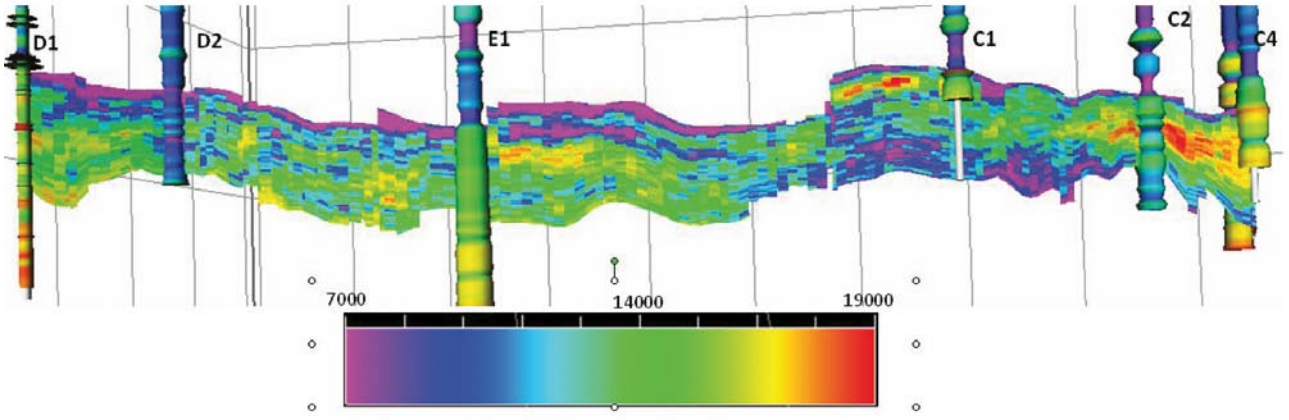

Figure 9 *Impedance derived from the stochastic inversion resampled to the geologic grid. The average cell thickness in the depth domain is about 5 m which corresponds approximately to 1 ms in the time domain.*

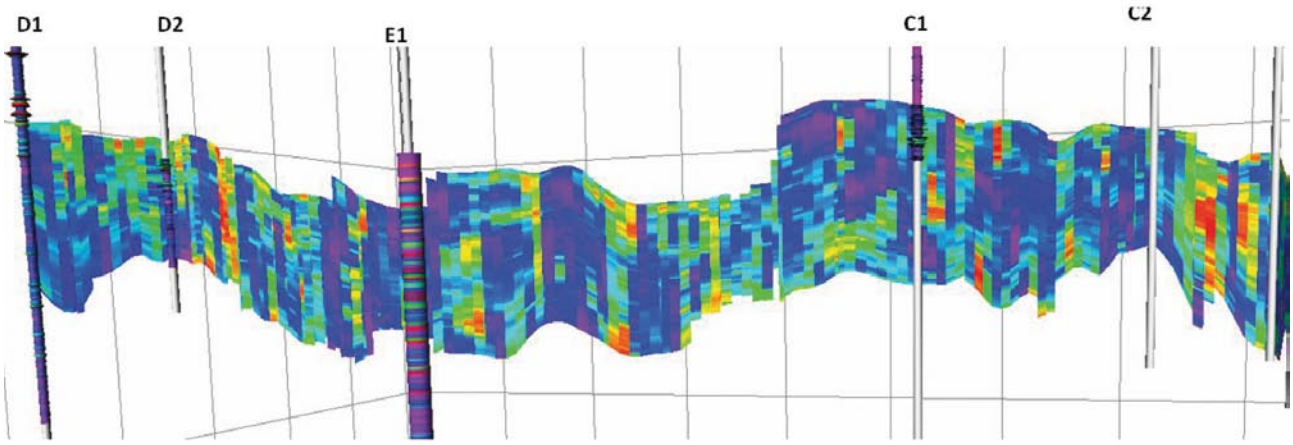

Figure 10 *Secondary porosity model derived using the sequential geologic modelling approach that relies on the neural network and uses as input a multitude of seismic attributes and geologic models derived in previous modelling steps. The green and red colours represent a high value of secondary porosity.*

Sequential geologic modelling

Given the availability of a large number of seismic attributes, the geologic modelling can be done in two different ways. One simple way is to use a geostatistical method, such as collocated co-kriging, or a sequential Gaussian simulation to incorporate one seismic attribute as soft information. Unfortunately, such methods cannot use all the seismic attributes simultaneously. Given that many seismic attributes contain valuable geologic information and could be very beneficial, the use of a neural network approach is more appropriate. In this project, a sequential geologic modelling approach (Ouenes et al. 2007) is used to estimate various geologic models.

The neural network will use the available well log data to find possible relationships between petrophysical properties and the multitude of available seismic attributes. Once these relationships are found with a subset of the well data during the training process, they will be tested on another subset not seen by the neural net during the training. The best neural network realizations able to have predictive capabilities on the testing subset are kept for further validation. Blind wells not used at all in the neural network training and testing process are used to select the best neural network realizations for prediction purposes.

In the considered carbonate field, the best well log properties are derived from the analysis of the image logs. The four major rock properties derived from the image logs are the total porosity, the secondary porosity, the connectedness, and the fracture density. In addition to these properties derived from the image logs, other conventional logs are used in the sequential geologic modelling. Fig. 10 shows the derived secondary porosity model which was estimated by using a multitude of seismic attributes and previously derived geologic models. After accumulating all possible and meaningful geologic models, the modelling of the fractures could be initiated.

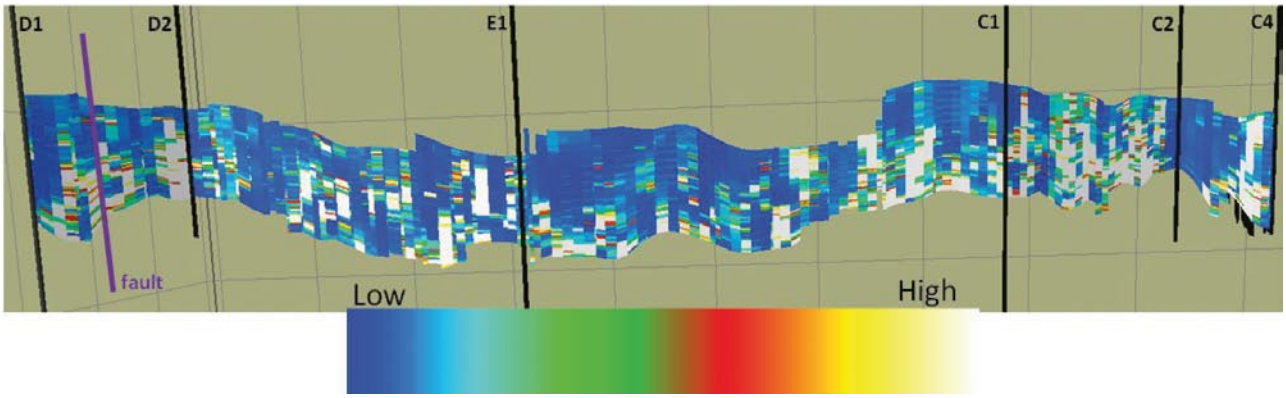

Figure 11 *Fracture density model derived using the CFM approach.*

Continuous fracture modelling (CFM)

The CFM approach does not attempt to extract fracture information from the seismic data itself, but rather uses the seismic data to estimate seismic attributes that have geologic meaning and represent fracture drivers that control where fracturing occurs. The same seismic attributes could also be used to derive seismically constrained geologic models such as total porosity that are known to be fracture drivers.

The CFM model uses the fracture density available at the wells and all the geophysical, and geologic drivers derived in the geophysical and geologic modelling. In this project, the estimation of the fracture density model used many post-stack seismic attributes, along with all the derived geologic models including gamma ray, total porosity, connectedness, and secondary porosity. All these drivers are available in 3D as geocellular models. Many fracture density realizations (Fig. 11) were generated, and they appear to be different from the models generated with other fracture modelling technologies (Akram et al., 2010).

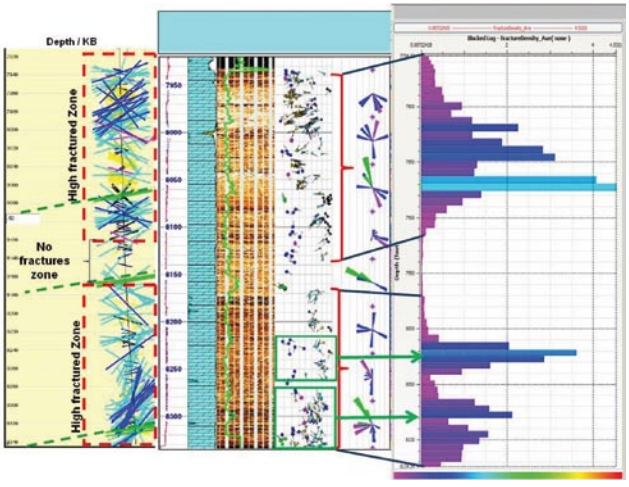

Figure 12 *Comparison between the predicted fracture density (on the right) with the interpreted FMI log (on the left). The model was able to capture the upper and lower fractured zones as well as the no fractured zone that separates them.*

One way to check the validity of the derived fracture density models is to test them in at least one blind well. To make the blind well test difficult, the most southerly well that exhibits different characteristics than the northern wells was selected as a blind well. A fracture density log was extracted at the blind well and compared to the actual fracture density. Fig. 12 shows the results of the blind well testing which indicated that the model was capable of predicting both the fractured and non-fractured zones. The comparison of the other logs (total porosity, secondary porosity) with the model predictions confirm the reliability of the approach and its predictive capabilities. These models were then used to plan two new wells. The results from one of the newly drilled wells are used as additional validation of the models.

Model validation with actual drilling

Based on the derived geologic and fracture models, well E2 was drilled in another fault compartment about 1 km south of E1. The position of E2 in Fig. 9 is on the right side of E1 where the stochastic inversion predicts the presence of two high porosity zones. This unique feature of two separate zones is only present in the fault block recently drilled with the E2 well. The actual drilling of well E2 did confirm the presence of these two zones and their high porosity. Fig. 13 shows the resistivity log which is able to pinpoint accurately the two zones. It is apparent that the derived geologic and

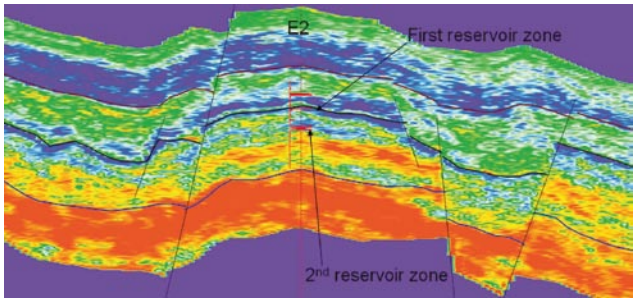

Figure 13 *Newly acquired resistivity log at well E2 showing the two zones as predicted by the stochastic impedance.*

fracture models have predictive capabilities as indicated by the blind well and confirmed by the actual drilling.

The use of an appropriate reservoir characterization workflow that relies heavily on post-stack seismic attributes derived from a narrow seismic survey enabled AGOCO to fully characterize the two most complex carbonate reservoir properties: vuggy porosity and fractures. These two reservoir properties entirely control the performance of the wells in the considered field. Using such advanced seismic and reservoir modelling technologies and workflows allows AGOCO to achieve success in its exploration efforts.

Acknowledgments

The authors wish to express their gratitude to the management of the exploration division of the Arabian Gulf Oil Company (AGOCO) and to Younis Faituri, for granting permission to publish this paper. Prism Seismic authors would like to thank their Libyan partner, Al Haram, for his continuing support and assistance.

References

Abadi. A., van Wees, J.D., van Dijk, P. and Cloetingh, S., [2008] Tectonics and Subsidence evolution of the Sirt Basin, Libya, *AAPG bulletin*, **92**, 8, 993-1027.

Akram, A.H., Gherryo, Y.S., Ali, S.M., Thabt, M.S. and Serban, A. [2010] Dynamic behavior of a fissured dual carbonate reservoir modeled with DFN. *SPE 127783*.

Al-Dosari S. and Marfurt, K. [2006] 3D volumetric multispectral estimates of reflector curvature and rotation. *Geophysics,* **71**(5), 41-P51.

Bejaoui, R. Ben Salem, R., Ayat H., Kooli, I., Balogh, D., Robinson, G., Royer, T., Boufares, T. and Ouenes, A., [2010] Characterization and simulation of a complex fractured carbonate field offshore Tunisia. *SPE 128417*.

Christensen, S.A., Ebbe Dalgaard, T., Rosendal, A., Christensen, J.W., Robinson, G., Zellou, A. and Royer, T, [2006] Seismically Driven Reservoir Characterization Using an Innovative Integrated Approach: Syd Arne Field. *SPE 103282*.

Cooke, D.A. and Schneider, W.A, [1983] Generalized linear inversion of reflection seismic data, *Geophysics,* **48**(6), 665-P 676.

Haas, A. and Dubrule, O. [1994], Geostatistical inversion: a sequential method of stochastic reservoir modelling constrained by seismic data. *First Break*, **12**(11), 561-569.

Jenkins, C., Ouenes, A., Zellou, A. and Wingard, J. [2009] Quantifying and predicting naturally fractured reservoir behavior with continuous fracture models. *AAPG Bulletin*, **93**, 11.

Lancaster, S. and Whitcombe, D. [2000] Fast track coloured inversion, SEG extended abstracts. *70th SEG Annual Meeting*, Calgary, Canada.

Laribi, M. et al. [2004] Integrated Fractured Reservoir Characterization and Simulation: Application to Sidi El Kilani Field, Tunisia. *Journal of Petroleum Technology*, August, and SPE 84455.

Mundim, E.C. Sohots, H.A., De Araujo, J.M. and Tavares, D.M, [2006] WT decon, a colored deconvolution implemented by wavelet transform. *The Leading Edge,* April.

Ouenes, A., Richardson, S. and Weiss, W. [1995] Fractured reservoir characterization and performance forecasting using geomechanics and artificial intelligence. *SPE 30572*.

Ouenes, A. [2000] Practical application of fuzzy logic and neural networks to fractured reservoir characterization, *Computers and Geosciences*, Shahab Mohagegh (Ed.) **26**, 7.

Ouenes, A. et al. [2007] Integrated Property and Fracture Modeling Using 2D Seismic Data: Application to an Algerian Cambrian Field. *SPE 109272*.

Ouenes, A. et al. [2008] Seismically Driven Characterization, Simulation and Underbalanced Drilling of Multiple Horizontal Boreholes in a Tight Fractured Quartzite Reservoir: Application to Sabria Field, Tunisia. *SPE 112853*.

Ouenes, A. et al. [2010] Integrated Characterization and Simulation of the Fractured Tensleep Reservoir at Teapot Dome for CO_2 Injection Design. *SPE 132404*.

Partyka, G., Gridley, J. and Lopez, J. [1999] Interpretational applications of spectral decomposition in reservoir characterization. *The Leading Edge*, **18**(3), 353-360.

Pinous, O. et al. [2006] Application of an Integrated Approach for Characterization of the Naturally Fractured Reservoir in The West Siberian Basement: Example of Maloichskoe Field. *SPE 102562*.

Ross, J.G, Zellou, A., Klepacki, D. [2009] Seismically driven fractured reservoir characterization using an integrated approach - Joanne Field, UK. *71st EAGE Annual Meeting,* Amsterdam.

Zellou, A., Robinson, G., Royer, T., Zahuczki, P. and Kiraly, A. [2006] Fractured reservoir characterization using post-stack seismic attributes: application to a Hungarian reservoir. *68th Annual EAGE Meeting*, Vienna, Austria.